Title

Autofluorescence-based analyses of intranuclear inclusions of Fragile X-associated tremor/ataxia syndrome

Journal

BioTechniques, 69(1)

ISSN

0736-6205

Authors

Ma, Lisa
Hagerman, Paul J

Publication Date

2020-07-01

DOI

10.2144/btn-2019-0144

Peer reviewed

HHS Public Access

Author manuscript

Biotechniques. Author manuscript; available in PMC 2021 July 01.

Published in final edited form as:

Biotechniques. 2020 July ; 69(1): 414–420. doi:10.2144/btn-2019-0144.

Autofluorescence-based Analyses of Intranuclear Inclusions of Fragile X-associated Tremor/Ataxia Syndrome

Lisa Ma[1], **Paul J Hagerman**[1],[2]

[1]Department of Biochemistry and Molecular Medicine, University of California Davis School of Medicine, Davis, California, USA

[2]MIND Institute, University of California Davis Health, Sacramento, California, USA

Abstract

Intranuclear inclusions present in Fragile X-associated tremor/ataxia syndrome (**FXTAS**) patient brains have historically been difficult to study due to their location and scarcity. The recent finding that these particles autofluoresce has complicated the use of immunofluorescence techniques, but also offers new opportunities for purification. We have ascertained the features of the autofluorescence, including its excitation/emission spectrum, similarities and differences compared to lipofuscin autofluorescence, and its presence/absence under various fixation, mounting, and UV light exposure conditions. Immunofluorescence at various wavelengths was conducted to determine which conditions are ideal for minimizing autofluorescence confounds. We also present a technique for autofluorescence-based sorting of FXTAS inclusions using flow cytometry, which will allow the field to more successfully purify inclusions for unbiased analyses.

Method summary

The intranuclear inclusions of FXTAS are autofluorescent across a broad range of wavelengths. We performed experiments using fluorescence microscopy to define the characteristics of this autofluorescence and to determine what immunofluorescence conditions might overcome interference from inclusion autofluorescence. The inclusion-associated autofluorescence pattern was also used to develop a method for purifying inclusions through nuclear isolation, sucrose fractionation, and fluorescence activated cell sorting.

Challenges of studying FXTAS inclusions

Fragile X-associated tremor/ataxia syndrome (**FXTAS**) is an X-linked neurodegenerative disease caused by a premutation CGG-repeat expansion (55–200 repeats) in the 5′ untranslated region of the *FMR1* gene. One of the hallmark features of this disease is the

Corresponding author: Paul J. Hagerman, MD, PhD.

Author contributions: LM and PJH were responsible for experimental concept and design. Fluorescence activated cell sorting was performed by the UC Davis Flow Cytometry Resource. All other material preparation, data collection, and analysis were performed by LM with support from PJH. The first draft of the manuscript was written by LM and both authors contributed to subsequent versions of the manuscript. Both authors read and approved the final manuscript.

Ethical disclosure: The authors state that they have obtained appropriate institutional review board approval or have followed the principles outlined in the Declaration of Helsinki for all human or animal experimental investigations. In addition, for investigations involving human subjects, informed consent has been obtained from the participants involved.

formation of intranuclear inclusions [1,2]. Studies on inclusion composition in inclusion disorders have always been challenging due to the difficulty in cleanly isolating inclusions. For many neurodegenerative inclusion disorders, inclusion formation is likely late stage and limited to the brain [3,4], and *in vitro* inclusion formation can never fully recapitulate formation *in vivo*. Therefore, samples are limited to *postmortem* human brain samples which are non-renewable, precious, and subject to deterioration. FXTAS inclusions are particularly challenging, as they are exclusively intranuclear, solitary, and only form in 2–20% of neurons and astrocytes [2]. Previous studies have relied on immunofluorescence to determine their composition [5–7]. However, immunofluorescence biases protein discovery and is not an accurate way to quantify protein levels.

Recently, FXTAS inclusions have been found to emit autofluorescence throughout a wide range of spectra [8], which interferes with immunofluorescence measurements for many wavelengths. A better alternative would be to isolate FXTAS inclusions for analysis. This has been attempted for other inclusion disorders, but methods generally rely on either antibody-based sorting or sequential extraction using detergents and chaotropes [9–12]. Antibody-based sorting introduces bias in the isolation process whereas sequential extraction assumes that all insoluble material is inclusion material, which may be inaccurate. As an alternative, we propose that immunofluorescence on FXTAS inclusions be performed according to guidelines that minimize interference from autofluorescence, and that FXTAS inclusions be sorted using autofluorescence-based strategies for optimal purity.

Features of FXTAS inclusion autofluorescence

To ensure that the autofluorescent particles observed are specifically inclusions, three FXTAS cases were scored using autofluorescence alone for inclusion load in the frontal cortex. Each case had at least 500 nuclei scored for inclusion presence. Inclusion loads for the three cases were 8.7%, 10.3%, and 14%, well within the range of previously estimates [2].

Frontal cortical nuclear smears prepared as previously described [10] were exposed to no stains or antibodies other than DAPI and were viewed under an upright fluorescence light microscope (Leica DM5500 B, Leica Microsystems, Buffalo Grove, IL). DAPI staining was necessary to provide nuclear context to identify which autofluorescent particles were inclusions, as lipofuscin was abundant in these samples. Approximately ten FXTAS samples identified through immunohistochemistry as patients with high inclusion loads were examined, and each exhibited inclusions autofluorescing weakly at 360nm and 620nm and strongly at 480nm and 545nm (Figure 1A). Since inclusions do not strongly autofluoresce at the wavelength in which DAPI is viewed, we do not believe DAPI staining significantly affected inclusion characterization. No autofluorescent intranuclear inclusions have been observed for control cases. Images were taken at 545nm at various exposure levels and magnifications to determine the lower limits of visual detection of inclusion autofluorescence, which was found to be 11.2ms at 60x magnification and 25.5ms at 100x magnification. Since exposure and wavelength heavily affect the intensity of viewable autofluorescence, we feel that both should be cited in future studies.

Identically prepared slides were also viewed on a stimulated emission depletion (**STED**) microscope with confocal capabilities (Leica SP8 STED 3x, Leica Microsystems, Buffalo Grove, IL), both to confirm that autofluorescence was visible using a separate microscope and to ascertain the specific excitation/emission properties of inclusion autofluorescence. Inclusion autofluorescence was apparent and was found to have maximal excitation/emission at 490nm/560nm, with an emission range from 475nm to 740nm, where emissions above 590nm gradually taper off in intensity (Figure 1B). The excitation/emission spectra of extranuclear lipofuscin autofluorescent particles on the same slide showed the same pattern of autofluorescence (Figure 1B). However, quantification of fluorescence intensity reveals that lipofuscin is significantly more intense at 545nm and 620nm (Figure 1C). These measured emission values correlate well with what is observable using light microscopy.

Additional slides were prepared using multiple fixation techniques to ensure that inclusion autofluorescence is not an artifact of slide preparation. FXTAS slides fixed using 3:1 methanol:acetic acid, 4% paraformaldehyde, Histochoice (VWR Amresco, Pennsylvania), and 70% methanol all exhibited autofluorescent inclusions (Figure 1D). Several different mountants have been tested, including Prolong Gold and Diamond Antifade Mountants and Slowfade Diamond Antifade Mountant (Thermo Fisher, Massachusetts), with no alterations in autofluorescent properties.

Inclusions were exposed to UV light to ascertain whether UV exposure could be used to remove the autofluorescence through photobleaching. FXTAS brain slides were incubated under long (365nm) and short wave (254nm) UV light for one hour then stained with DAPI and compared to untreated slides. Neither condition significantly altered the autofluorescence intensity of the inclusions, although the short-wave light damaged the DNA enough to preclude DAPI staining (Figure 1E). This indicates that UV exposure would not be a viable method to avoid autofluorescence interference.

Optimized strategies for performing immunofluorescence on FXTAS inclusions

To demonstrate the best combination of fluorophores and exposures that may be used to avoid autofluorescence interference, FXTAS frontal cortical nuclear slides were prepared using ubiquitin and SUMO 2/3 primary antibodies in combination with secondary antibodies bound to Alexa-488, Alexa-555, and Alexa-647 (Thermo Fisher, Massachusetts). Ubiquitin and SUMO 2/3 are present at high levels in FXTAS inclusions [8] and therefore have a higher chance of producing strong enough immunofluorescence signals to overcome the effect of autofluorescence. When inclusion immunofluorescence was performed using the ubiquitin antibody at 480nm, no difference in fluorescence intensity was seen in comparison to inclusion autofluorescence at 480nm (Figure 2A). SUMO 2/3 immunofluorescence at 480nm produced the same result (Figure 2A). At 545nm, ubiquitin inclusion immunofluorescence did not display brighter intensity over inclusion autofluorescence. On the other hand, SUMO 2/3 immunofluorescence was significantly brighter than inclusion autofluorescence at the same wavelength (Figure 2B). (Figure 2B). The wavelength which best avoids interference from autofluorescence is 647nm, where both ubiquitin and SUMO

2/3 immunofluorescence produced a significantly brighter signal in comparison to autofluorescence at the same wavelength (Figure 2C). Whenever possible, immunofluorescence on FXTAS inclusions should be performed in this region of the spectrum.

The discrepancy between ubiquitin and SUMO 2/3 immunofluorescence at 545nm illustrates the need to validate each new antibody used for immunofluorescence, especially if the wavelength used is not in the far-red spectrum. Immunofluorescence results can vary widely depending on the amount of a protein present in inclusions, the quality of the antibody used, and the immunofluorescence protocol, so new conditions should always be re-determined. Secondary only controls should be presented alongside immunofluorescence images to serve as comparison, and exposure levels, gains, and wavelength should be reported for transparency. Inclusion proteins identified using immunofluorescence prior to the discovery of autofluorescence (i.e. lamin A/C, hnRNPs, SAM68, FMRpolyG, LAP2β, TRA2A, etc.) may have, in fact, been at least partially artifactual. However, given the limitations to conducting immunofluorescence on FXTAS inclusions, rather than use immunofluorescence to re-validate these proteins, we instead conducted mass spectrometry in a separate publication [8] to ascertain their presence and relative abundance. Most of these proteins were found to be present in inclusions, but some at extremely low abundance, which highlights the need to follow specific guidelines when conducting inclusion immunofluorescence.

Autofluorescence-based flow cytometry activated cell sorting (FACS) of inclusions

Although autofluorescence presents an impediment to conducting immunofluorescence, it provides a unique opportunity in terms of inclusion isolation. FACS based on the autofluorescence signal of the inclusions avoids the antibody-based bias and sequential extraction inaccuracies that have hampered previous isolation attempts. Since lipofuscin exhibits a similar pattern of autofluorescence, brain samples must first undergo a nuclear isolation to eliminate as much lipofuscin as possible. 1g of pulverized fresh frozen frontal cortex from FXTAS patients was Dounce homogenized with a loose pestle on ice using a modified protocol from Iwahashi 2006 [10], and ultracentrifugation in a sucrose buffer as described by McEwen and Zigmond 1972 [13] allowed for a sufficiently clean nuclear isolation. Nuclei were then placed on top of a continuous sucrose gradient and ultracentrifuged again, producing a band of inclusion-enriched particles at a density corresponding to about 1.30 g/ml. The band was absent in control samples.

The inclusion-enriched fractions from seven FXTAS samples were then used for FACS alongside four identically prepared control sample fractions. Inclusions were identified in FXTAS samples as particles that upon excitation using a 488nm laser, emitted strong green to orange fluorescence (500–565nm), but weak red fluorescence (>670nm) (Figure 3A). Other laser lines at 405nm, 561nm, and 640nm were also assessed before 488nm excitation was determined to be optimal. Since inclusions are smaller subcellular particles, logarithmic scaling was used on the detectors for laser light scattering, as is customary in the field of

flow cytometry [14], and larger aggregates with significantly longer laser dwell rates were eliminated. Sorted inclusions were viewed by fluorescence light microscopy and found to exhibit the same fluorescence pattern exhibited by in situ inclusions (Figure 3B). Sorted inclusion samples have an estimated purity level of 80–90%, and this technique was successfully used for mass spectrometry analysis of FXTAS inclusions [8].

Altogether, these results demonstrate that although inclusion autofluorescence calls for more stringent guidelines when performing immunofluorescence studies, it also generates new opportunities for cleanly purifying inclusions for unbiased analytical approaches. There are still improvements that can be made, as the method for purifying inclusions through FACS is time intensive, requires large amounts of brain, and does not produce samples of 100% purity. More work can also be done to evaluate the levels of proteins that must be present within an inclusion for immunofluorescence to produce a signal high enough to overcome autofluorescence. However, these methods pave the way to allow FXTAS researchers to delve deeper into the mechanics behind inclusion formation, which can offer insights into the pathogenesis of neurodegenerative inclusion disorders.

Ethical conduct of research

All procedures performed in studies involving human participants were in accordance with the ethical standards of the institutional and/or national research committee (UCD Institutional Review Board; protocol #215292) and with the 1964 Helsinki declaration and its later amendments or comparable ethical standards. Written Informed consent was obtained from all individual participants or their family designates included in the study.

Acknowledgements:

The authors wish to acknowledge the help of Bridget McLaughlin, Technical Director of the UC Davis (**UCD**) Flow Cytometry Resource. Assistance was also provided by Ingrid Brust-Mascher at the Health Sciences District Advanced Imaging Facility at UCD using the Leica SP8 STED 3x. The authors also acknowledge the assistance of Dr. Veronica Martinez-Cerdeno with the Department of Pathology and Laboratory Medicine at UCD for dissecting the brain samples.

Financial disclosures: The authors declare that they have no competing interests. This project was supported by the UCD Flow Cytometry Shared Resource Laboratory with funding from the NCI P30 CA093373 (Cancer Center) and S10 OD018223 (Astrios Cell Sorter) grants, with technical assistance from Bridget McLaughlin and Jonathan Van Dyke. This study was partially funded by the Yearlong Exposure to Advanced Research training program (LM) under grant numbers T32OD010931 and the Marjorie and Charles Elliott Fellowship offered by the UCD Integrative Genetics and Genomics Graduate Group. This work was also supported by NIH grant GM113929 (PJH).

References

1. Hagerman RJ, Hagerman P. Fragile X-associated tremor/ataxia syndrome — features, mechanisms and management. Nat. Rev. Neurol 12(7), 403–412 (2016). [PubMed: 27340021]
2. Greco CM, Berman RF, Martin RM, et al. Neuropathology of fragile X-associated tremor/ataxia syndrome (FXTAS). Brain. 129(1), 243–255 (2006). [PubMed: 16332642]
3. Jellinger KA. Interaction between α-Synuclein and Other Proteins in Neurodegenerative Disorders [Internet]. Sci. World J (2011). Available from: https://www.hindawi.com/journals/tswj/2011/371893/.
4. Zarouchlioti C, Parfitt DA, Li W, Gittings LM, Cheetham ME. DNAJ Proteins in neurodegeneration: essential and protective factors. Philos. Trans. R. Soc. B Biol. Sci 373(1738), 20160534 (2018).

5. Buijsen RA, Sellier C, Severijnen L-AW, et al. FMRpolyG-positive inclusions in CNS and non-CNS organs of a fragile X premutation carrier with fragile X-associated tremor/ataxia syndrome. Acta Neuropathol. Commun. [Internet] 2 (2014). Available from: https://www.ncbi.nlm.nih.gov/pmc/articles/PMC4254384/.

6. Cid-Samper F, Gelabert-Baldrich M, Lang B, et al. An Integrative Study of Protein-RNA Condensates Identifies Scaffolding RNAs and Reveals Players in Fragile X-Associated Tremor/Ataxia Syndrome. Cell Rep. 25(12), 3422–3434.e7 (2018). [PubMed: 30566867]

7. Sellier C, Buijsen RAM, He F, et al. Translation of Expanded CGG Repeats into FMRpolyG Is Pathogenic and May Contribute to Fragile X Tremor Ataxia Syndrome. Neuron. 93(2), 331–347 (2017). [PubMed: 28065649]

8. Ma L, Herren AW, Espinal G, et al. Composition of the Intranuclear Inclusions of Fragile X-associated Tremor/Ataxia Syndrome. Acta Neuropathol. Commun 7(1), 143 (2019). [PubMed: 31481131]

9. Kametani F, Obi T, Shishido T, et al. Mass spectrometric analysis of accumulated TDP-43 in amyotrophic lateral sclerosis brains. Sci. Rep. [Internet] 6 (2016). Available from: https://www.ncbi.nlm.nih.gov/pmc/articles/PMC4793195/.

10. Iwahashi CK, Yasui DH, An H-J, et al. Protein composition of the intranuclear inclusions of FXTAS. Brain. 129(1), 256–271 (2006). [PubMed: 16246864]

11. Tanaka G, Yamanaka T, Furukawa Y, Kajimura N, Mitsuoka K, Nukina N. Biochemical and morphological classification of disease-associated alpha-synuclein mutants aggregates. Biochem. Biophys. Res. Commun 508(3), 729–734 (2019). [PubMed: 30528390]

12. McCormack A, Keating DJ, Chegeni N, Colella A, Wang JJ, Chataway T. Abundance of Synaptic Vesicle-Related Proteins in Alpha-Synuclein-Containing Protein Inclusions Suggests a Targeted Formation Mechanism. Neurotox. Res 35(4), 883–897 (2019). [PubMed: 30796693]

13. McEwen BS, Zigmond RE. Isolation of Brain Cell Nuclei [Internet] In: Research Methods in Neurochemistry: Volume 1 Marks N, Rodnight R (Eds.), Springer US, Boston, MA, 139–161 (1972) [cited 2019 Jun 14]. Available from: 10.1007/978-1-4615-7748-5_6.

14. Petersen TW, Brent Harrison C, Horner DN, van den Engh G. Flow cytometric characterization of marine microbes. Methods. 57(3), 350–358 (2012). [PubMed: 22796378]

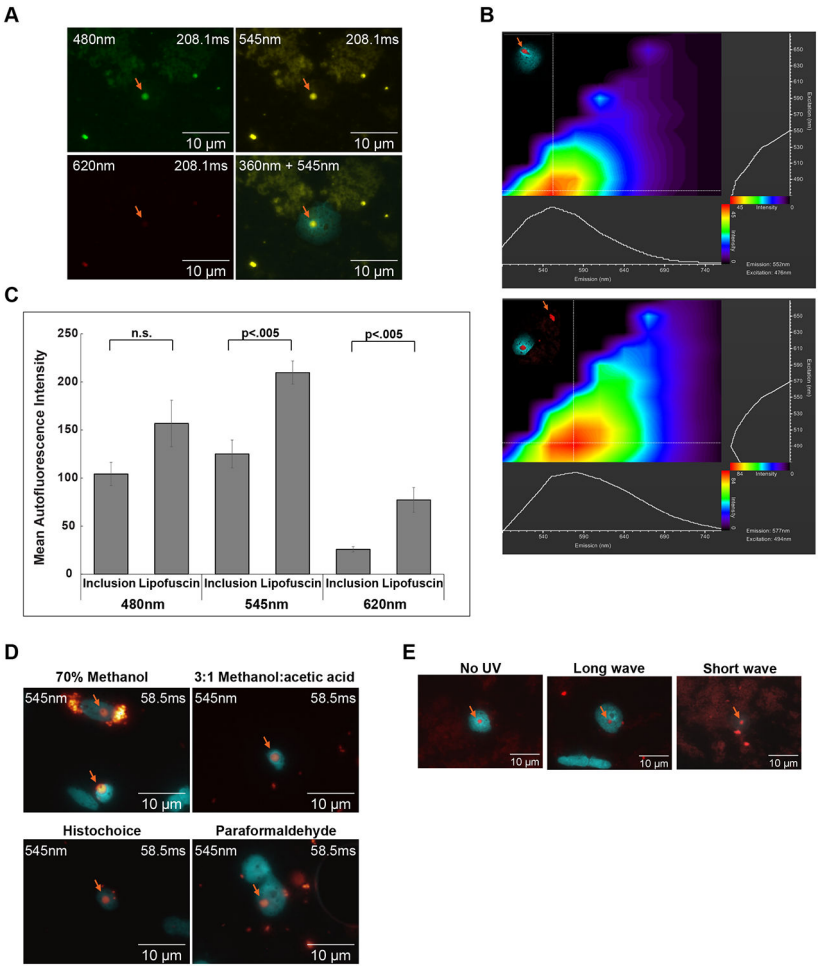

Figure 1:

A: FXTAS inclusions autofluoresce strongly at 480nm and 545nm and weakly at 360nm and 620nm. Nuclei isolated from FXTAS post-mortem frontal cortex tissue were fixed using 70% methanol and stained with DAPI only then examined at various wavelengths. Images were taken at 100x. Orange arrows denote inclusions. Wavelength (nm) and exposure level (ms) used to create the images are indicated, respectively, in the upper left and upper right corners of the image.

B: FXTAS inclusions exhibit maximal excitation/emission spectra at 490nm/560nm. Lipofuscin exhibits similar maximal excitation/emission spectra, but higher relative emission intensities at far red wavelengths. FXTAS isolated brain nuclei slides stained with DAPI were analyzed on a stimulated emission depletion (STED) microscope for autofluorescence excitation/emission spectra. Inclusions were found to have maximal excitation/emission at 490nm/560nm, with an emission range from 475nm to 740nm, where emissions above 590nm gradually taper off in intensity. Autofluorescent lipofuscin particles on the same slide show similar patterns of autofluorescence, except they show higher intensities of emission in far red wavelengths. Orange arrows denote the object that is being measured. Figure adapted from Reference 8, 2019, with permission from Creative Commons Attribution 4.0 International License https://creativecommons.org/licenses/by/4.0/.

C: FXTAS inclusion and lipofuscin autofluorescence differ significantly in intensity. Mean autofluorescence intensities were measured for inclusions from four different FXTAS patients along with lipofuscin found in the same images. Lipofuscin displays significantly higher autofluorescence levels at both the 545nm and 620nm wavelengths. Figure adapted from Reference 8, 2019, with permission from Creative Commons Attribution 4.0 International License https://creativecommons.org/licenses/by/4.0/.

D: FXTAS inclusions exhibit the same pattern of autofluorescence under all examined fixation methods. FXTAS isolated brain nuclei were fixed using four different fixation methods and stained with DAPI only, then examined at 545nm under fluorescent light microscope. Images were taken at 100x. DAPI staining is displayed in cyan and autofluorescence at 545nm is displayed in red. Orange arrows point to inclusions. Wavelength (nm) and exposure level (ms) used to create the images are indicated, respectively, in the upper left and upper right corners of the image.

E: FXTAS inclusions do not exhibit photobleaching after long and short-wave UV exposure. FXTAS isolated brain nuclei slides were exposed to either no UV light, long wave 365nm UV light, or short wave 254nm UV light for 1 hour, then stained with DAPI before imaging at 480nm. Images were taken at 60x with an exposure of 208.1ms. No condition eradicated inclusion autofluorescence upon visual inspection or significantly decreased it.

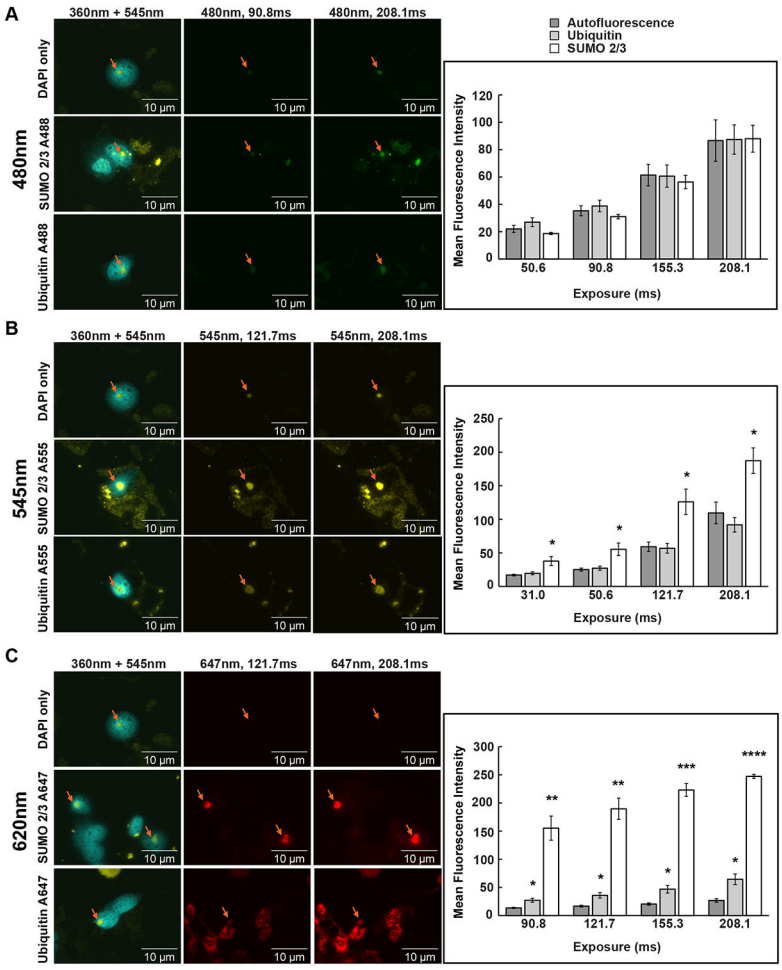

Figure 2:

A: Ubiquitin staining and SUMO 2/3 staining at 480nm are not significantly brighter than inclusion autofluorescence. Orange arrows denote inclusions. No significant differences were found.

B: Ubiquitin staining at 545nm is not significantly brighter than inclusion autofluorescence, but SUMO 2/3 staining is. Orange arrows denote inclusions.

*Significant difference from the autofluorescence bar with $p<0.05$

C: Both ubiquitin staining and SUMO 2/3 staining at 647nm are significantly brighter than inclusion autofluorescence. Orange arrows denote inclusions.

*Significant difference from the autofluorescence bar with $p<0.05$

**$p<0.005$

***$p<0.0005$

****$p<5\times105$

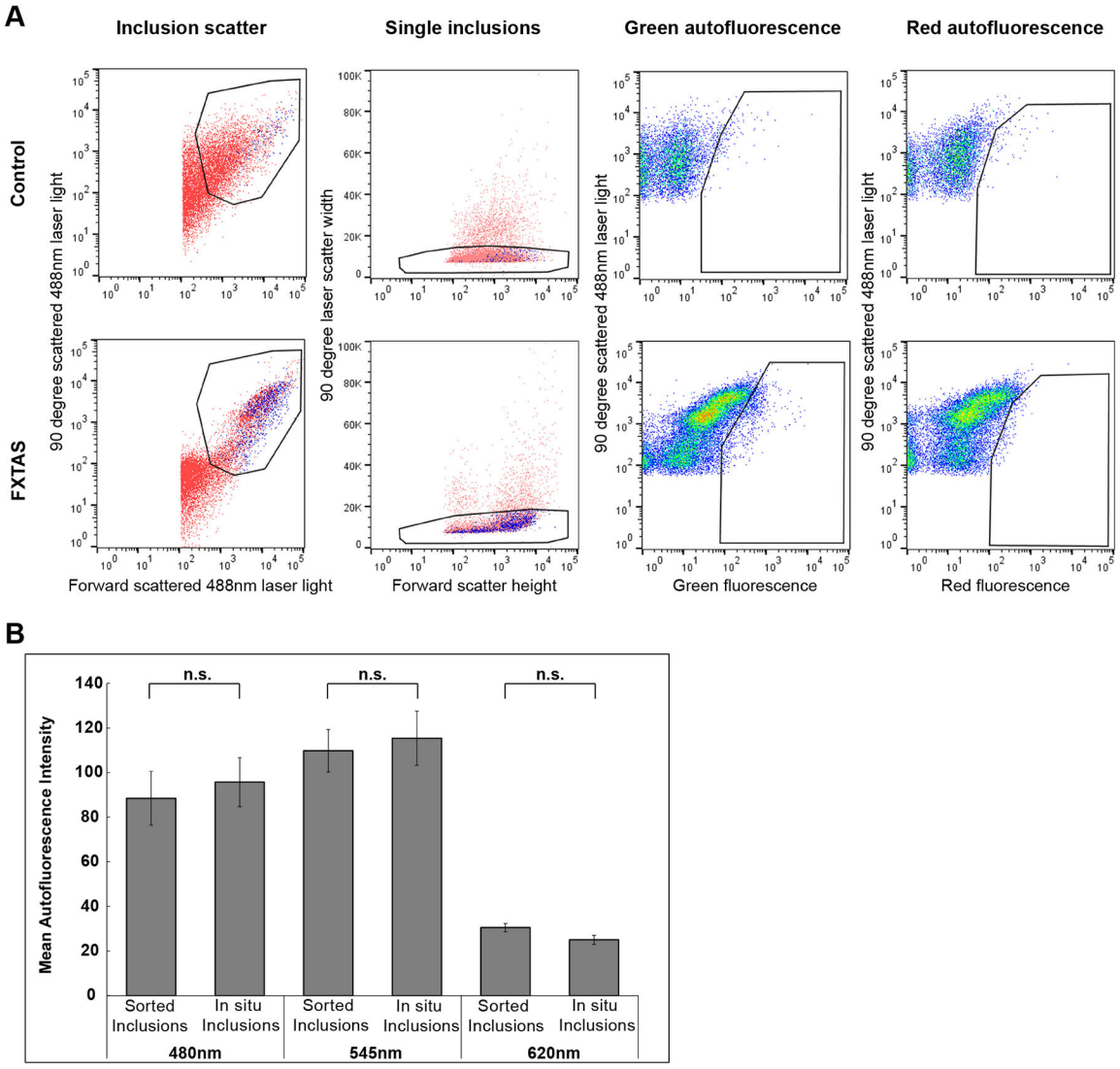

Figure 3:

A: Inclusion-enriched fractions used in FACS contain a population of FXTAS-specific particles identified by size and fluorescence properties. Logarithmic scaling was used on the detectors assigned to laser light scatter measurements ("Inclusion scatter"), and larger aggregates were removed by plotting the duration of 90° laser light scatter to remove objects with markedly increased laser dwell rates relative to the shorter transit times of single particles ("Single inclusions"). Sorted particles were identified as a population in FXTAS samples that was absent in control samples which exhibited strong green fluorescence emission and weak red fluorescence emission (gates in "Green autofluorescence" and "Red autofluorescence", respectively). Figure reprinted from Reference 8, 2019, with permission from Creative Commons Attribution 4.0 International License https://creativecommons.org/licenses/by/4.0/.

B: Flow sorted FXTAS inclusions are indistinguishable from in situ FXTAS inclusions as viewed by immunofluorescence. Inclusions sorted by flow cytometry were verified by microscopic analysis to confirm that sorted inclusions exhibit the same properties as FXTAS

inclusions viewed in situ. Mean autofluorescence intensities for in situ FXTAS inclusions and sorted inclusions were measured at 3 different wavelengths, and no significant difference was found for any of the wavelengths measured. Figure reprinted from Reference 8, 2019, with permission from Creative Commons Attribution 4.0 International License https://creativecommons.org/licenses/by/4.0/.